VIP *The following Communications have been judged by at least two referees to be "very important papers" and will be published online at www.angewandte.org soon:*

*H. Jiang, P. Elsner, K. L. Jensen, A. Falcicchio, V. Marcos, K. A. Jørgensen**
Achieving Molecular Complexity by Organocatalytic One-Pot Strategies: A Fast Entry for the De Novo Synthesis of Sphingoids, Amino Sugars, and Polyhydroxylated α-Amino Acids

*T. J. Kucharski, Z. Huang, Q.-Z. Yang, Y. Tian, N. C. Rubin, C. D. Concepcion, R. Boulatov**
Kinetics of Thiol/Disulfide Exchange Correlates Weakly with the Restoring Force in the Disulfide Moiety

*W. Xu, X. Xue, T. Li, H. Zeng, X. Liu**
Ultrasensitive and Selective Colorimetric DNA Detection by Nicking Endonuclease-Assisted Nanoparticle Amplification

H. Ueda, H. Satoh, K. Matsumoto, K. Sugimoto, T. Fukuyama, H. Tokuyama**
Total Synthesis of (+)-Haplophytine

G. A. Zelada, J. Riu, A. Düzgün, F. X. Rius**
Immediate Detection of Living Bacteria at Ultra-Low Concentrations Using a Carbon-Nanotube-Based Potentiometric Aptasensor

*K. Fuchibe, T. Kaneko, K. Mori, T. Akiyama**
Expedient Synthesis of N-Fused Indoles: A C–F Activation and C–H Insertion Approach

A. Giannis, P. Heretsch, V. Sarli, A. Stößel*
Synthesis of Cyclopamine Using a Biomimetic and Diastereoselective Approach

*W. A. Chalifoux, R. McDonald, M. J. Ferguson, R. R. Tykwinski**
***tert*-Butyl Endcapped Polyynes: Crystallographic Evidence of Reduced Bond-Length Alternation**

*S. T. Scroggins, Y. Chi, J. M. J. Fréchet**
Polarity-Directed One-Pot Asymmetric Cascade Reactions Mediated by Two Catalysts in an Aqueous Buffer

News


J.-P. Behr


K. S. Schanze


A. Boldyrev

Books

Highlights

Synthetic Methods

Radicals and Transition-Metal Catalysis: An Alliance Par Excellence to Increase Reactivity and Selectivity in Organic Chemistry

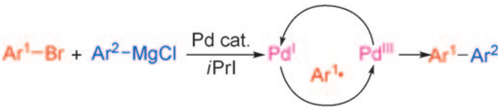

Welcome to radical catalysis: Radicals are "tamed" in transition-metal complexes which serve as catalysts for a number of reactions—Kumada couplings (see scheme), highly regioselective cobalt-catalyzed eliminations, Markovnikov additions, and reductive epoxide openings catalyzed by a titanium/rhodium system. All of these reactions are powered by the high reactivity of radical intermediates in the catalytic cycle of the metal-catalyzed process.

Divergent Reactions

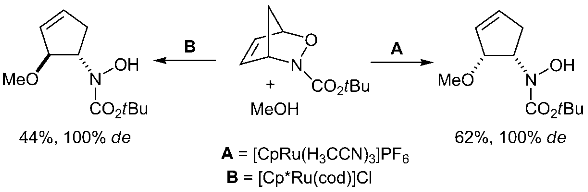

Either–or: Exciting developments have been made in the field of transition-metal-catalyzed ring-opening reactions of bicyclic, heteroatom-containing Diels–Alder adducts. These regio- und stereodivergent reactions open interesting new alternatives to conventional methods (see scheme, cod = 1,5-cyclooctadiene).

Drug Discovery in Insects

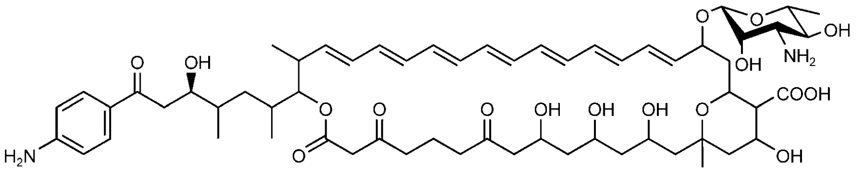

candicidin D

Candicidin D is a potent natural product that was recently re-isolated from bacterial insect symbionts. Some insects cultivate the producing bacteria in specialized organs in order to fight pathogens. Besides the identification of new natural products for human use, these findings have also implications for our understanding of resistance development and drug discovery strategies in general.

Minireviews

Atropisomerism

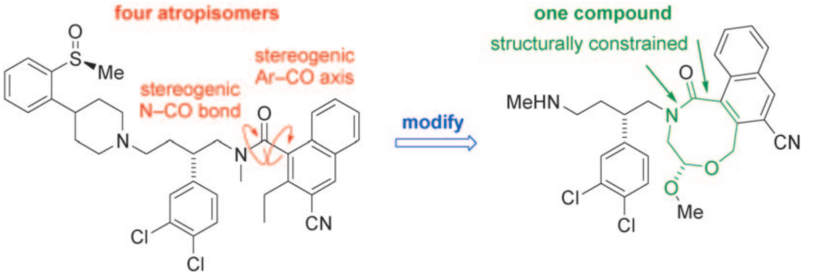

A twist in the tale: Recent reports have highlighted solutions to the problems encountered when drug candidates exist as slowly interconverting conformers or atropisomers (see scheme). This Minireview brings together the various strategies that have been adopted and proposes a general approach to handling an aspect of stereochemistry which has received little attention from drug regulatory agencies.

For the USA and Canada: ANGEWANDTE CHEMIE International Edition (ISSN 1433-7851) is published weekly by Wiley-VCH, PO Box 191161, 69451 Weinheim, Germany. Air freight and mailing in the USA by Publications Expediting Inc., 200 Meacham Ave., Elmont, NY 11003. Periodicals postage paid at Jamaica, NY 11431. US POSTMASTER: send address changes to *Angewandte Chemie*, Wiley-VCH, 111 River Street, Hoboken, NJ 07030. Annual subscription price for institutions: US$ 7225/6568 (valid for print and electronic / print or electronic delivery); for individuals who are personal members of a national chemical society prices are available on request. Postage and handling charges included. All prices are subject to local VAT/sales tax.

Reviews

Molecular Spectroscopy

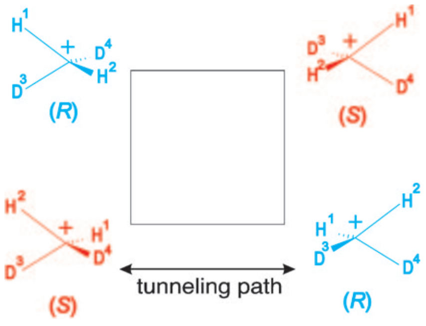

More than distortion: The Jahn–Teller effect in molecules is more complex than a simple geometric distortion. It significantly alters the electronic and geometric structure, and can result in unexpected isomerism and chirality, for example in deuterated isotopologues of CH_4^+ (see picture). Rotationally resolved photoelectron spectroscopy and group theory provide precise information about the dynamic structure of Jahn–Teller distorted molecules.

Communications

Nanotubes

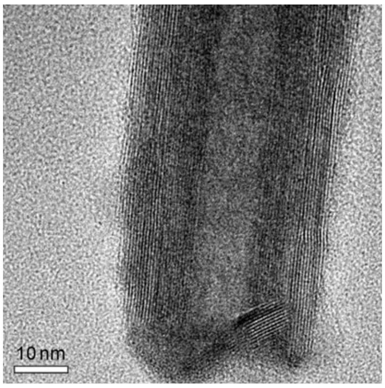

Nanotubes of tin disulfide were fabricated from SnS_2 nanoflakes by the vapor–liquid–solid process using bismuth nanodroplets as a catalyst. The SnS_2 reagent in the gas phase preferentially adsorbs onto the bismuth particles; upon cooling, nucleation and growth of SnS_2 nanotubes occurs (see HRTEM image). Annealing the nanotubes results in the formation of SnS_2/SnS superlattices.

Polymer-Peptide Conjugates

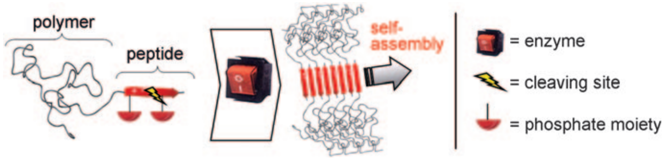

At the flick of a switch: Introducing phosphate moieties into $(Thr\text{-}Val)_X$ peptide aggregation domains disturbs the formation of secondary structures. This suppression is used to regulate the self-assembly of polymer–peptide conjugates. A phosphatase enzyme which hydrolyzes the phosphate esters then triggers the self-assembly process generating fibrillar aggregates (see scheme).

Zintl Anions

Zintl to the third: $[Zn@Zn_5Sn_3Bi_3@Bi_5]^{4-}$ (see structure), the first ternary intermetalloid Zintl anion, was obtained upon reaction of the binary anion $[Sn_2Bi_2]^{2-}$ with $ZnPh_2$ in 1,2-diaminoethane/[2.2.2]crypt solution. X-ray structure analysis and DFT calculations indicate varied bonding within the intermetalloid cage and rationalize the impact of the ternary composition on structural and electronic properties.

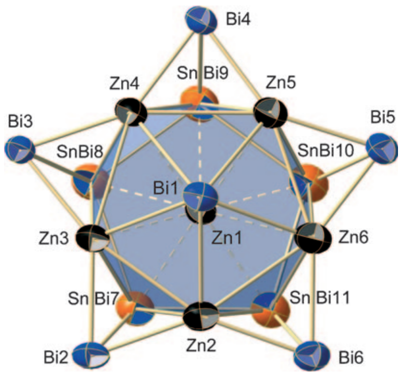


A Journal of the Gesellschaft Deutscher Chemiker
Angewandte
International Edition
GDCh
D 3461
Chemie
www.angewandte.org
2008–47/5
WILEY-VCH

Interfaces

S. Sen, S. Yamaguchi,
T. Tahara* ______________ **6439 – 6442**

Different Molecules Experience Different Polarities at the Air/Water Interface

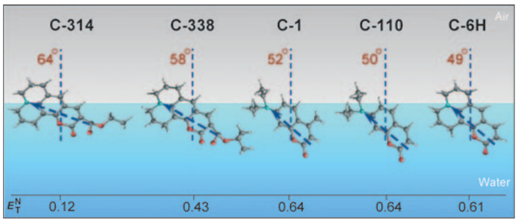

Split the difference: Interface-selective nonlinear spectroscopy disclosed that five coumarin derivatives exhibit significantly different solvachromatic shifts at the air/water interface, revealing that structurally different molecules experience notably different local effective polarities (E_T^N), even at the same water interface (see picture; arrows indicate transition dipole moments).

Peptide Rotaxanes

A. Fernandes, A. Viterisi, F. Coutrot,
S. Potok, D. A. Leigh,* V. Aucagne,*
S. Papot* ______________ **6443 – 6447**

Rotaxane-Based Propeptides: Protection and Enzymatic Release of a Bioactive Pentapeptide

Ring of protection: A [2]rotaxane **1** protects and selectively releases a bioactive pentapeptide. The rotaxane macrocycle provides a defensive shield that very significantly improves the poor stability of the peptide to both individual peptidases and the cocktail of enzymes present in human plasma. Glycosidase-catalyzed cleavage of a carbohydrate 'stopper' in the rotaxane triggers release of the parent peptide (see picture).

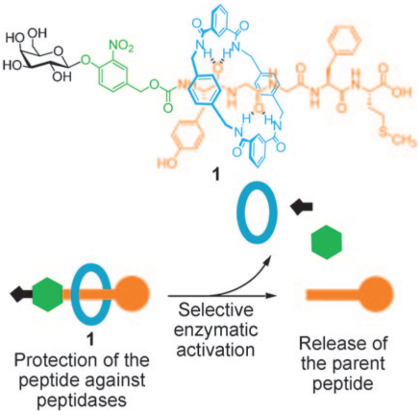

Antitumor Agents

H.-J. Lee, N. X. Wang, D.-L. Shi,*
J. J. Zheng* ______________ **6448 – 6452**

Sulindac Inhibits Canonical Wnt Signaling by Blocking the PDZ Domain of the Protein Dishevelled

A new application: The nonsteroidal anti-inflammatory drug sulindac interacts directly and specifically with the PDZ domain of the protein Dishevelled (Dvl), which is a key intracellular component of the Wnt signaling pathways. Sulindac binds to the conventional peptide-binding pocket of the domain (see picture), and may exert a cancer chemoprotective effect by blocking it, thereby inhibiting canonical Wnt signaling.

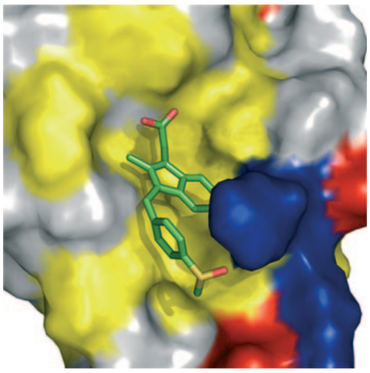

Metallacycles

T. Wang, S. Li, H. Zhang, R. Lin, F. Han,
Y. Lin, T. B. Wen, H. Xia* ____ **6453 – 6456**

Annulation of Metallabenzenes: From Osmabenzene to Osmabenzothiazole to Osmabenzoxazole

$[Os]=[Os(PPh_3)_2(NCS)_2]^-$

Fused metallaaromatics have been conveniently prepared from metallabenzenes (see scheme). The intramolecular S_NAr reaction of an osmabenzene allowed the first examples of a metallabenzothiazole and a metallabenzoxazole to be isolated.

H_2 Activation

T. Hiromoto, E. Warkentin, J. Moll,
U. Ermler, S. Shima* ——— **6457 – 6460**

The Crystal Structure of an [Fe]-Hydrogenase–Substrate Complex Reveals the Framework for H_2 Activation

An open and closed case: The structure of a binary complex of C176A [Fe]-hydrogenase with methylenetetrahydromethanopterin was solved at 2.15 Å resolution in an open conformation. A closed form of the complex was modeled on the basis of the experimentally determined structure. In this model, the iron-site *trans* to the acyl carbon is located next to the C14a and therefore considered as H_2 binding site.

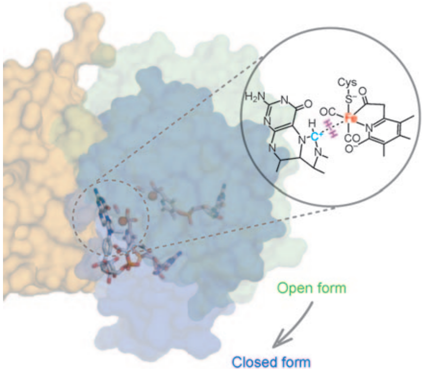

Artificial Photosynthesis

R. Bhosale, A. Perez-Velasco,
V. Ravikumar, R. S. K. Kishore, O. Kel,
A. Gomez-Casado, P. Jonkheijm,
J. Huskens, P. Maroni, M. Borkovec,
T. Sawada, E. Vauthey,* N. Sakai,*
S. Matile* ——— **6461 – 6464**

Topologically Matching Supramolecular n/p-Heterojunction Architectures

Matching matters when building supramolecular n/p-heterojunction photosystems on solid supports that excel with efficient photocurrent generation, important critical thickness, smooth surfaces, and flawless responsiveness to functional probes for the existence of operational intra- and interlayer recognition motifs.

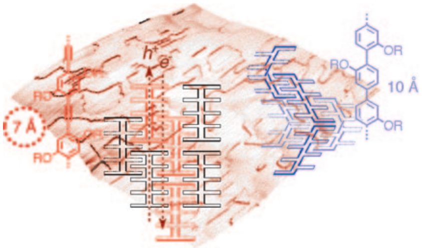

VIP

Glycome Analysis

W. Cheng, L. Ding, S. J. Ding, Y. B. Yin,
H. X. Ju* ——— **6465 – 6468**

A Simple Electrochemical Cytosensor Array for Dynamic Analysis of Carcinoma Cell Surface Glycans

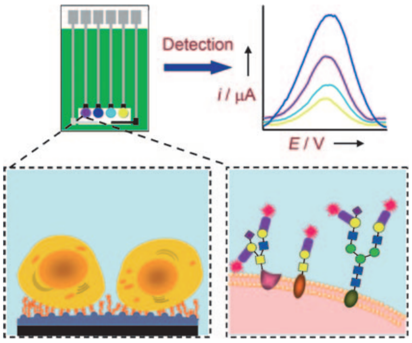

Sugar and spice: The title method for the simultaneous multiplex analysis of intact cell-surface glycans (see picture) shows excellent performance in sensitivity, stability, and practicality. The strategy can be used to analyze the dynamic variation of the cell-surface glycome and to decipher cellular pathophysiological processes.

Bond Theory

S. C. A. H. Pierrefixe, S. J. M. van Stralen,
J. N. P. van Stralen, C. Fonseca Guerra,
F. M. Bickelhaupt* ——— **6469 – 6471**

Hypervalent Carbon Atom: "Freezing" the S_N2 Transition State

High Five! Under certain circumstances a carbon atom can become hypervalent (see structure) and bind five substituents in the trigonal-bipyramidal structure, which is normally the labile S_N2 transition state.

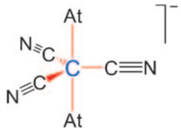

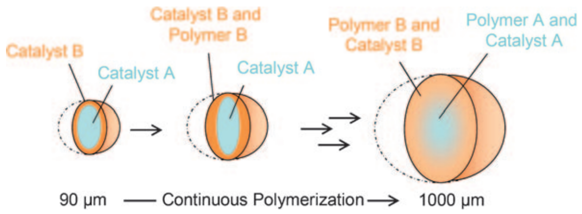

Two in one: A replication effect allows the formation of core–shell particles in a single olefin polymerization step, which occurs through the simultaneous use of spatially resolved metallocene catalysts immobilized on a hybrid inorganic–organic support (see picture). Catalyst A was exclusively supported in the inorganic core, while catalyst B was immobilized in the organic shell.

Core–Shell Particles

T. Diesing, G. Rojas, M. Klapper,* G. Fink, K. Müllen* ______ **6472 – 6475**

Spatially Resolved Catalysis for Controlling the Morphology of Polymer Particles

---

Small but important: A miniaturized prototype for pH sensing in the pH range 5–7.5 has been constructed from a photoluminescent Eu^{3+} metal–organic framework that contains two different Eu^{3+} sites (Eu1 and Eu2; see picture) and self-assembles through hydrogen bonding and π–π interactions. This material has a very high quantum yield and an excellent balance between absorption, energy transfer, and emission rate.

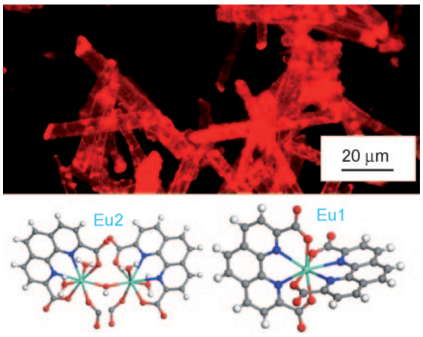

Lanthanides

B. V. Harbuzaru, A. Corma,* F. Rey, J. L. Jordá, D. Ananias, L. D. Carlos, J. Rocha* ______ **6476 – 6479**

A Miniaturized Linear pH Sensor Based on a Highly Photoluminescent Self-Assembled Europium(III) Metal–Organic Framework

---

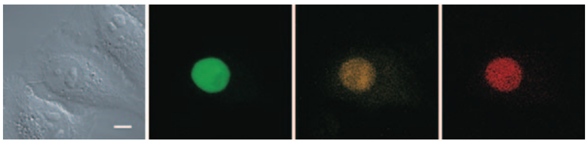

A colorful bunch: A series of fluorescent probes designed on the basis of fluorescence quenching caused by an excitonic interaction contain different dye moieties and fluoresce in various colors upon hybridization with their target nucleic acid. The picture shows simultaneous fluorescence in three colors in the nucleus of a cell containing an excess of three different microRNA strands. Left: differential interference contrast image.

Fluorescent Probes

S. Ikeda, T. Kubota, M. Yuki, A. Okamoto* ______ **6480 – 6484**

Exciton-Controlled Hybridization-Sensitive Fluorescent Probes: Multicolor Detection of Nucleic Acids

---

Carbon-coated Sn nanoparticles in carbon nanofibers (see image) were fabricated by pyrolysis of coaxially electrospun nanofibers as an anode material for Li-ion batteries. The significantly improved electrochemical performance of such an electrode is believed to result from the unique nanostructure consisting of a thin carbon shell around tin nanoparticles, which are further encapsulated in hollow carbon nanofibers.

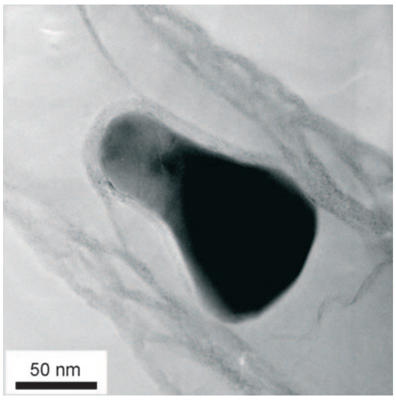

Nanotechnology

Y. Yu,* L. Gu,* C. Wang, A. Dhanabalan, P. A. van Aken, J. Maier ______ **6485 – 6489**

Encapsulation of Sn@carbon Nanoparticles in Bamboo-like Hollow Carbon Nanofibers as an Anode Material in Lithium-Based Batteries

Contents

POM-Based Nanocomposites

C. Streb, R. Tsunashima, D. A. MacLaren, T. McGlone, T. Akutagawa, T. Nakamura, A. Scandurra, B. Pignataro, N. Gadegaard, L. Cronin* ______ **6490 – 6493**

Supramolecular Silver Polyoxometalate Architectures Direct the Growth of Composite Semiconducting Nanostructures

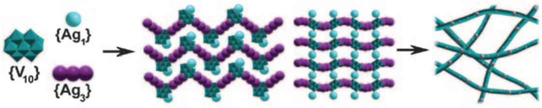

Nanosilver on a string: Crystalline silver polyoxovanadate supramolecular architectures are employed as precursors for the synthesis of composite nanowires (see scheme). The nanostructures are composed of semiconducting vanadium oxide which forms wires with high aspect ratios, and are embedded with metallic silver nanoparticles.

Drug Delivery

Z. Cao, R. Tong, A. Mishra, W. Xu, G. C. L. Wong,* J. Cheng,* Y. Lu* ______ **6494 – 6498**

Reversible Cell-Specific Drug Delivery with Aptamer-Functionalized Liposomes

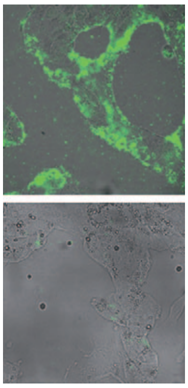

Aptamer advantages: Cell-specific delivery of the anticancer drug cisplatin through a nucleolin-aptamer-conjugated, cisplatin-encapsulating liposome delivery system is described. Calcein was incorporated into the target MCF-7 cells (see top image) but not into LNCaP cells (see bottom image). More importantly, the extent of delivery can be controlled by using a complementary DNA of the aptamer as an antidote.

Ionomers

S. Gu, R. Cai, T. Luo, Z. Chen, M. Sun, Y. Liu, G. He, Y. S. Yan* ______ **6499 – 6502**

A Soluble and Highly Conductive Ionomer for High-Performance Hydroxide Exchange Membrane Fuel Cells

Easy cell: The new polymeric ionomer TPQPOH with a tris(2,4,6-trimethoxyphenyl)phosphonium unit has excellent solubility in some low-boiling-point water-soluble solvents, high ionic conductivity, and outstanding alkaline stability. A hydroxide exchange membrane fuel cell containing this ionomer exhibits increased peak power density and reduced internal resistance.

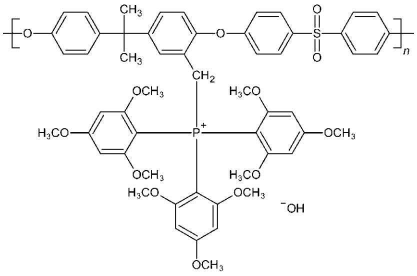

TPQPOH

Asymmetric Catalysis

W.-J. Liu, B.-D. Lv, L.-Z. Gong* ______ **6503 – 6506**

An Asymmetric Catalytic Darzens Reaction between Diazoacetamides and Aldehydes Generates *cis*-Glycidic Amides with High Enantiomeric Purity

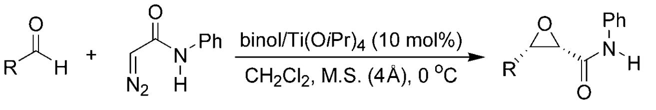

up to > 99% *ee*
28 examples

Titanium strength: The title reaction was catalyzed by a chiral titanium complex formed in situ from commercially available Ti(O*i*Pr)$_4$ and (*R*)-binol, and gave *cis*-glycidic amides with excellent enantiomeric purity (see scheme). This new method has been applied to the preparation of chiral building blocks used for the synthesis of the side chain of taxol and (−)-bestatin.

Total Synthesis

T. J. Donohoe,* A. Flores, C. J. R. Bataille, F. Churruca ______ **6507 – 6510**

Synthesis of (−)-Hygromycin A: Application of Mitsunobu Glycosylation and Tethered Aminohydroxylation

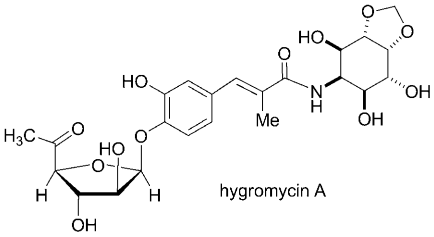

Key points in the synthesis of (−)-hygromycin A are the tethered aminohydroxylation reaction used to prepare the aminocyclitol unit and the choice of a bulky protecting group on the sugar unit to facilitate selective Mitsunobu glycosylation and also bestow kinetic stability upon an otherwise vulnerable proton.

C−H Alkenylation

A. García-Rubia, R. G. Arrayás,* J. C. Carretero* ______ **6511 – 6515**

Palladium(II)-Catalyzed Regioselective Direct C2 Alkenylation of Indoles and Pyrroles Assisted by the *N*-(2-Pyridyl)sulfonyl Protecting Group

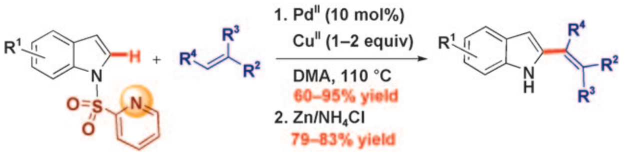

Easy on, easy off: The *N*-(2-pyridyl)sulfonyl group controls the direct Pd^{II}-catalyzed alkenylation of indoles, affording the corresponding products in good yields and with complete regiocontrol at C2 (see scheme, DMA = dimethylacetamide). The protocol was also extended to pyrrole derivatives. The final reductive desulfonylation affords the C2-substituted indoles and pyrroles in good yields.

Liquid Crystals

S. Castellanos, F. López-Calahorra, E. Brillas, L. Juliá,* D. Velasco* ______ **6516 – 6519**

All-Organic Discotic Radical with a Spin-Carrying Rigid-Core Showing Intracolumnar Interactions and Multifunctional Properties

The discotic liquid crystal radical 1, which is very stable in the solid state or solution, has an enantiotropic ordered hexagonal columnar mesophase above room temperature with magnetic interactions among molecular spins. Radical **1** shows electrochemical amphotericity and absorption and light-emission properties that cover the red region of the visible spectrum.

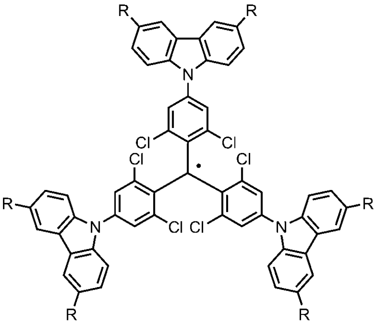

1: R= COC$_{17}$H$_{35}$

Tandem Reactions

L. Zhao, F. Xie, G. Cheng, Y. Hu* ______ **6520 – 6523**

A Base-Promoted Tandem Reaction of 3-(1-Alkynyl)chromones with 1,3-Dicarbonyl Compounds: An Efficient Approach to Functional Xanthones

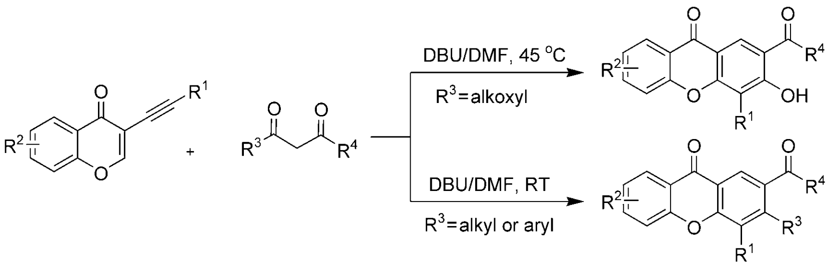

No need for a transition-metal catalyst is characteristic for the tandem process presented herein to obtain functionalized xanthones. The sequence involves multiple reactions, such as Michael addition-elimination/cyclization/1,2-addition/elimination reactions (see scheme).

Asymmetric Catalysis

C. Wang, C. Q. Li, X. F. Wu, A. Pettman,
J. L. Xiao* ______ **6524 – 6528**

pH-Regulated Asymmetric Transfer Hydrogenation of Quinolines in Water

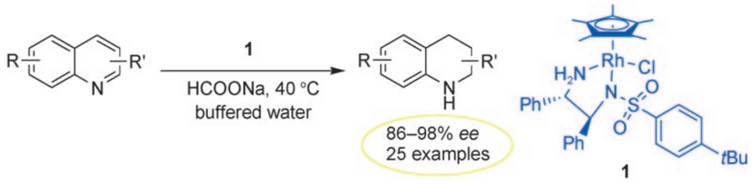

In buffered water, a broad range of quinoline derivatives underwent asymmetric transfer hydrogenation in air with the rhodium catalyst **1** and sodium formate as the hydrogen source to furnish synthetically important 1,2,3,4-tetrahydroquinolines with excellent enantioselectivities (see scheme; R = H, Me, F, Cl, Br, OMe; R′ = alkyl, aryl).

Biomass Conversion

L. Deng, J. Li, D.-M. Lai, Y. Fu,*
Q.-X. Guo* ______ **6529 – 6532**

Catalytic Conversion of Biomass-Derived Carbohydrates into γ-Valerolactone without Using an External H_2 Supply

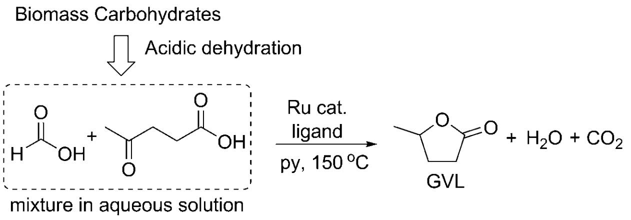

Simplified procedure: A new catalytic route was developed for the conversion of biomass carbohydrates into γ-valerolactone (GVL) without using an external H_2 supply. A model experiment with glucose provided γ-valerolactone in 48 % yield. An interesting positive effect of CO_2 on the Ru-catalyzed hydrogenation was also observed. py = pyridine.

Microfabrication

S. Ota, S. Yoshizawa,
S. Takeuchi* ______ **6533 – 6537**

Microfluidic Formation of Monodisperse, Cell-Sized, and Unilamellar Vesicles

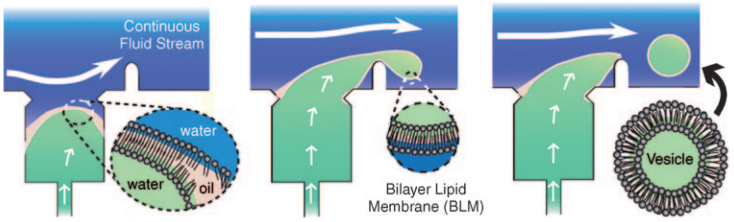

Gently down the stream: A microfluidic technique uses a continuous fluid stream to generate monodisperse unilamellar phospholipid vesicles from a single bilayer (see picture). Since the vesicles are robust and efficiently encapsulate high concentrations of various molecules, they are useful as delivery vehicles and as model cellular systems.

Polyoxometalates

J. M. Pigga, M. L. Kistler, C.-Y. Shew,*
M. R. Antonio,* T. Liu* ______ **6538 – 6542**

Counterion Distribution around Hydrophilic Molecular Macroanions: The Source of the Attractive Force in Self-Assembly

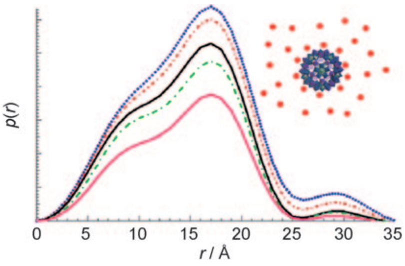

Growing blackberries: The association of counterions around $\{Mo_{72}V_{30}\}$ polyoxometalate macroanions increases with increasing macroion concentration and decreasing solvent polarity. The counterion distribution extends about 2–9 Å from the macroion surface with the highest probability at 2–3 Å from the macroion surface. A close connection between counterion association and the self-assembly of $\{Mo_{72}V_{30}\}$ into “blackberry” structures is observed.

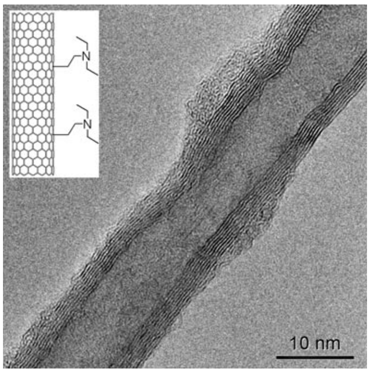

Graft it! Target active sites were directly grafted onto structural defects of carbon nanotubes (see picture) by electrophilic attack. This synthetic route is faster and more efficient than other approaches, and it allows a single-site design of carbon nanotube-based heterogeneous catalysts. The potential of such catalysts is tremendous for liquid-phase biomass conversion reactions.

Functionalized Nanotubes

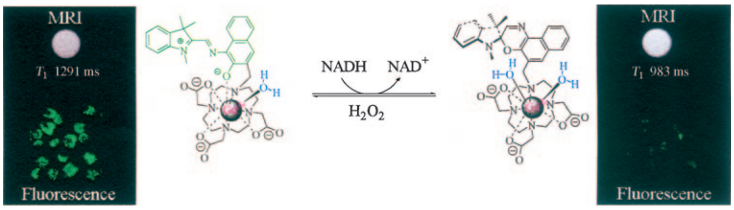

Agents get smart: A macrocycle-based gadolinium complex undergoes an isomerization in the presence of NADH, leading to an r_1 relaxivity increase of 54 %, while the intense fluorescence disappears (see scheme). This agent could facilitate the use of magnetic resonance imaging (MRI) for probing tissue redox status.

MRI Agents

Self-help groups: The aluminatopyrrolyl complexes $[\{\eta^5\text{-}2,3,4,5\text{-}Me_4C_4N\text{-}(AlClMe_2)\}_2Cr]$ and $[\{\eta^5\text{-}2,3,4,5\text{-}Me_4C_4N\text{-}(AlClMe_2)CrMe(\mu\text{-}NPh)_2AlMe_2\}\{Me_3Al\text{-}(thf)\}]$ self-activate to give single-site ethylene polymerization catalysts. The closely related dinuclear chromium(II) complex $[\{\eta^5\text{-}2,3,4,5\text{-}Me_4C_4N\text{-}(AlClMe_2)Cr\}_2(\mu\text{-}Me)_2]$ (see picture) is a highly active self-activating ethylene trimerization catalyst.

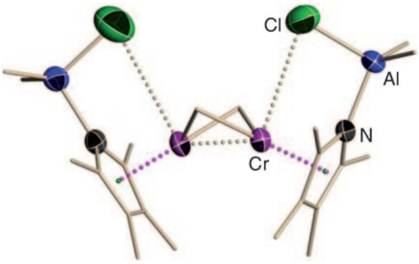

Ethylene Polymerization

Supporting information is available on www.angewandte.org (see article for access details).

A video clip is available as Supporting Information on www.angewandte.org (see article for access details).

Service